

## Article

# Esterification and Transesterification Optimization Processes of Nonedible (Castor and Neem) Oils for the Production of Biodiesel

Hamid Ayyub <sup>1</sup>, Muhammad Arslan <sup>1</sup>, Muhammad Jamshaid <sup>1,\*</sup> , Akbar Ali Qureshi <sup>1</sup> , Arslan Ahmed <sup>2</sup>,  
Haji Hassan Masjuki <sup>3</sup>, Md. Abul Kalam <sup>4,\*</sup> , Farah Binti Ahmad <sup>5</sup> , Hafiz Liaqat Ali <sup>1</sup>,  
Muhammad Umair Ahsan Khan <sup>1</sup> and Muhammad Umer Khallidoon <sup>1</sup> 

<sup>1</sup> Department of Mechanical Engineering, Faculty of Engineering and Technology, Bahauddin Zakariya University, Multan 60000, Pakistan; engrhamidmech@gmail.com (H.A.); marslankhan8010@gmail.com (M.A.); akbaraliqureshi@bzu.edu.pk (A.A.Q.); liaqatali@bzu.edu.pk (H.L.A.); umair.ahsan@bzu.edu.pk (M.U.A.K.); umarkhalidoon@gmail.com (M.U.K.)

<sup>2</sup> Department of Mechanical Engineering, COMSATS University Islamabad, Wah Campus 46000, Pakistan; arslanahmad@ciitwah.edu.pk

<sup>3</sup> Department of Mechanical Engineering, Faculty of Engineering, IIUM, Kuala Lumpur 50728, Malaysia; masjuki@iium.edu.my

<sup>4</sup> School of Civil and Environmental Engineering, FEIT, University of Technology Sydney, Ultimo, NSW 2007, Australia

<sup>5</sup> Department of Chemical Engineering and Sustainability, Faculty of Engineering, IIUM, Kuala Lumpur 50728, Malaysia; farahahmad@iium.edu.my

\* Correspondence: muhammad.jamshaid@bzu.edu.pk (M.J.); mdabul.kalam@uts.edu.au (M.A.K.)

**Abstract:** In current times, the diminishing reserves of petroleum, increased energy consumption across various sectors, and their consequential environmental impact have become apparent. Consequently, it is necessary to develop sustainable and eco-friendly energy sources to meet growing demands. The article aimed to blend castor and neem oils (in a 50:50 ratio) to rectify the drawbacks present in castor biodiesel such as elevated kinematic viscosity and density. Response surface methodology was used to study the optimization of the two-step biodiesel production process through the use of a central composite design (CCD). For the esterification step, a methanol-to-oil molar ratio of 7.5:1, 1.75 wt.% of H<sub>2</sub>SO<sub>4</sub>, and a temperature of 55 °C were optimal. In the transesterification step, optimized conditions included a methanol-to-oil molar ratio of 9:1, 2.50 wt.% of calcium oxide, a temperature of 55 °C, and a stirring speed of 900 rpm, resulting in a 93% yield of methyl ester. Different properties of produced biodiesel were examined using the standard values provided by EN 14214 and ASTM D6751. The production of biodiesel from a mixture of castor and neem oils did not have any adverse impacts on food security.

**Keywords:** esterification; transesterification; response surface methodology; biodiesel; castor oil; neem oil



**Citation:** Ayyub, H.; Arslan, M.; Jamshaid, M.; Qureshi, A.A.; Ahmed, A.; Masjuki, H.H.; Kalam, M.A.; Ahmad, F.B.; Ali, H.L.; Khan, M.U.A.; et al. Esterification and Transesterification Optimization Processes of Nonedible (Castor and Neem) Oils for the Production of Biodiesel. *Fuels* **2024**, *5*, 782–802. <https://doi.org/10.3390/fuels5040043>

Academic Editor: Maria A. Goula

Received: 30 July 2024

Revised: 9 September 2024

Accepted: 7 November 2024

Published: 12 November 2024



**Copyright:** © 2024 by the authors. Licensee MDPI, Basel, Switzerland. This article is an open access article distributed under the terms and conditions of the Creative Commons Attribution (CC BY) license (<https://creativecommons.org/licenses/by/4.0/>).

## 1. Introduction

The significance of fossil fuels has been enhanced exponentially in the modern era, where a variety of industries are being run on fossil fuels, which is essential for the growth of the economy [1]. However, immense usage has resulted in a significant decline of non-renewable resources; additionally, environmental factors like global warming have prompted global phenomena, and there have been a lot of studies on alternative fuels in recent years [2,3]. To substitute fossil fuels, experts are searching for and creating alternative energy sources in light of the current deteriorating scenario, putting an emphasis on sustainability and environmental friendliness. Researchers are developing more efficient ways to produce energy from green and renewable sources, including solar, wind, hydro, and tidal. However, it is still challenging to meet the requirements of replacing traditional fossil fuels. So, in order to live in the current depreciating condition, feasible renewable

green fuels are required. The commonly utilized biofuels, including biodiesel, bioethanol, and biogas, can serve as potential alternative fuels to overcome the energy demand [4]. The triglycerides found in vegetable oil react with alcohols and other substances to create fatty acid esters known as alkyl esters, which are the building blocks of biodiesel. Transesterification is a simple and affordable process for producing biodiesel. Biodiesel can be considered a significant advancement in renewable energy technologies due to its non-toxic and biodegradable properties.

Additionally, its combustion produces minimal greenhouse gas emissions and generates negligible amounts of hazardous environmental pollutants as compared to diesel petroleum [5,6]. Because biodiesel is such a potent medium, it can be mixed in different ratios with petroleum diesel fuel to make different blends [7]. The process of the transesterification of vegetable and animal fat triglycerides yields biodiesel. Beyond its advantages, producing biodiesel fuel has a number of challenges. The physiochemical properties of feedstocks, such as moisture content, free fatty acid content, and fatty acid composition, have an impact on the process and final product of biodiesel production. For instance, the fuel properties of biodiesel, such as oxidative stability, cetane number, cloud point, flash point, and heat content, are influenced by the chain length and unsaturation of the component fatty acids. Alkali catalysts need a lot of carbinol and are extremely sensitive to water and free fatty acids.

Additionally, alkali catalysts cause a saponification reaction, which complicates the process of separating glycerin and biodiesel. The fundamental catalyst reacts with these free fatty acids, causing soap production and the loss of some of the catalyst's capacity for transesterification. The creation of gels during the soap-making process also increases viscosity [8]. The majority of the first-generation feedstocks, which are edible oils used to make biodiesel such as canola, soybean, palm and rapeseed oils, sparked market conflict between food and fuel. Due to their low FFA concentration and high biodiesel output with an alkali catalyst, the edible oils served as the significant feedstock for the amalgamation of biodiesel [9].

Moreover, the cost of feedstock oil is estimated to range from seventy to ninety percent of the cost of producing biodiesel [10]. Blended fuels (B5, B10, B20) are made by combining biodiesel with petroleum diesel fuel. These blended fuels can be used in diesel engines without engine modifications instead of biodiesel (B100) [11].

The previous reports reveal that the biodiesel synthesized from animal fat and vegetable oils can have an adverse impact on the performance parameters of the diesel engine components, such as the injection system, combustion mechanism, and corrosion in the tanks. Due to the high oxygen concentration in biodiesel, biodiesel emits higher NO<sub>x</sub> content compared to petroleum diesel. Vehicle materials (brass and copper) are susceptible to corrosion from biodiesel, which can result in deposits at injection pumps, fuel system obstructions, seal failures, and filter clogging [12]. Several initiatives have employed blended feedstocks in their projects, combining edible and nonedible oils, edible and edible oils, as well as nonedible and nonedible oils. To counteract the drawbacks of using a single feedstock, several types of oil feedstocks are now being mixed. Even under the same process circumstances, biodiesel made from a combination of oils had a higher quality than biodiesel made from a single feedstock [13]. Researchers proposed various remedies for addressing the difficulties caused by the competing elements affecting the price of biodiesel and the limitations associated with the widespread utilization of single oil feedstocks. Among these solutions, the recommendation to blend oils in a suitable proportion before the transesterification process is highlighted as a valuable technique. This approach is suggested to effectively address issues such as feedstock shortages and the suboptimal quality of fuel [14,15]. In a one study, Wancura J.H. et al. [16] stated that related to the biodiesel, the yield was influenced by the composition of the oils when beef tallow and soybean oils were combined. The biodiesel yield was observed to be 79.9% when beef tallow and soybean oils were used as the feedstock. O.A. Falowo et al. [17] reported that it was found that converting the mixture of rubber seed oil and neem oil into biodiesel yielded

an impressive 98.7% and declared that the fuel's properties fulfilled ASTM requirements. Sharma et al. [18] reported that ternary oil mixtures made from Karanja, jatropha, and cottonseed, and quaternary oil mixtures made from Karanja, jatropha, coconut, and palm were also used to make biodiesel. T.F. Adepoju et al. [19] stated that in using a combination of pig and neem seed oil to generate biodiesel, they achieved the 98.03% (highest) yield by having a 60:40 mixing ratio for these oils. M.A. Mujtaba et al. [20] reported that they created biodiesel through the transesterification of palm and sesame oils using methanol. By employing the same proportion of sesame oil as palm oil, they attained a biodiesel yield of 96.61%. S. Niju et al. [21] reported that in another investigation, the combination of *Calophyllum inophyllum* oil and WCO resulted in a 96.5% (highest) conversion rate. D. Kumar et al. [22] stated that castor oil and Karanja oil were also combined to produce biodiesel, and a 78% (the highest) yield was acquired. A.B. Fadhil et al. [23] stated that radish seed oil and prunus apricot kernel oil were found to produce high-quality biodiesel in large quantities, with outstanding yields of 94.2% when combined.

In biodiesel production, the catalyst is crucial. There have been reports of a variety of catalysts, including enzymes and homogeneous and heterogeneous catalysts. The enzyme catalysts do not saponify and do not require a complex purification process because they are insensitive to free fatty acids. However, there are a number of issues with enzymes, including the inhibitory effect when employing methanol and the humongous enzyme cost with an extended time of reaction [24]. In general, homogeneous catalysts are inexpensive and very effective. However, removing them from the reaction mixture can be both time consuming and costly.

Additionally, their neutralization generates a significant volume of wastewater [25]. It has been determined that heterogeneous catalysts are helpful because they prove advantageous due to their ability to demonstrate elevated activity even in temperate reaction conditions, and the procedures for separating and reutilizing materials are comparatively uncomplicated [26]. According to studies, switching from homogeneous to heterogeneous catalysts can lower manufacturing costs by 4% to 20% and make processes simpler [27].

This research study was conducted to produce biodiesel by combining castor oil (*Ricinus communis*) and neem oil (*Azadirachta indica*). The goal of the article was to make a blend of castor and neem oils (in a 50:50 ratio) to rectify the drawbacks present in castor biodiesel, such as elevated kinematic viscosity and density. Previous research indicated that the heterogeneous catalyst CaO was never employed to make biodiesel with a mixture of castor and neem oils; CaO is a highly effective heterogeneous catalyst. The evaluation of biodiesel yield was conducted by examining the impact of various process input parameters. These parameters encompassed catalyst dosage, alcohol-to-oil molar ratio, reaction temperature, and reaction duration. Response surface methodology was used to optimize process parameters. Fuel properties such as density, kinematic viscosity, cetane number, acidic value, and calorific value of the castor oil and neem oil mixture were investigated and compared to EN 14214 and ASTM D 6571 standards. The production of biodiesel from a blend of castor oil and neem oil did not have any adverse impacts on food security. Interest in biodiesel has grown as more people look for a fuel that can be used as an alternative to petroleum diesel fuel. While biodiesel is a fuel with many benefits, there are certain health risks as well. According to the research literature, using biodiesel increases NO<sub>x</sub> emissions, which can lead to a number of health issues, including headaches, respiratory irritation, lung edema, emphysema, eye irritations, appetite loss, and tooth erosion. Children, asthmatics, and those suffering from chronic bronchitis, emphysema, or other respiratory conditions make up the majority of those afflicted [28].

## 2. Materials and Methods

### 2.1. Materials

Castor oil and neem oil were acquired from Multan, Pakistan. Various materials like beakers, conical flasks, volumetric flasks, thermometers, distilled water, and diamond aluminum foil were used in the present study. Chemicals used for biodiesel production,

such as sulfuric acid (99% pure), methanol (99% pure), calcium oxide (catalyst), and anhydrous sodium sulfate were purchased from local market suppliers in Pakistan. Sulfuric acid and methanol were used in the esterification process, while the transesterification process involved the use of calcium oxide and methanol to produce biodiesel. The acidic value of the oil mixture (castor and neem oil) before the esterification process was 14.36 mg of KOH/g oil.

## 2.2. Preparation of Oil Mixture

In this study, the blend of two distinct oils, namely castor oil and neem oil, was made in a proportion of (50:50). The blending process was carried out utilizing a magnetic stirrer hot plate, which was run for 30 min at 650 RPM to ensure that the oils were thoroughly mixed, and a uniform mixture was achieved. Once the homogeneous blend was obtained, it served as the input needed to make biodiesel [29].

## 2.3. Biodiesel Production

### 2.3.1. Esterification Process

The esterification process for the mixture of castor and neem oils was indispensable for generating biodiesel. In order to avoid soap formation and guarantee the manufacture of high-quality biodiesel, this procedure attempted to reduce the amount of free fatty acids present. The mixture of castor and neem oils was first heated separately on a magnetic stirrer hot plate to elevate the oil mixture's temperature according to the suggested design of experiment (DOE) temperature mentioned in Table 5, and then put into an esterification apparatus. Subsequently, a prescribed quantity of catalyst  $H_2SO_4$  was first shifted into a measuring glass cylinder, and then the catalyst was incorporated into the esterification apparatus. In this way, we used the acid as a catalyst, and this process was called esterification. The other parameters values, such as catalyst concentration and methanol-to-oil molar ratio, were also altered for each experiment according to the amounts mentioned in the DOE. Each experiment lasted for 90 min to guarantee the thorough disintegration of every component of free fatty acids [30]. The solution was allowed to cool briefly at room temperature once the reaction was finished. Once the esterification process was finalized, the mixture was moved to a separating funnel and retained within it for up to 24 h. This interval facilitated the settling of impurities like surplus methanol and unreacted catalysts, which settled at the funnel's base. After 24 h, the solution had separated into two layers: glycerol was present in the bottom layer (impurities), while the upper layer comprised esterified oil. Ultimately, the esterified oil mixture was decanted from the separation funnel into a flask for subsequent utilization in the transesterification process.

### 2.3.2. Transesterification Process

After obtaining a homogeneous mixture of oils, the mixture was preheated to perform the transesterification process to produce biodiesel according to the steps mentioned in Figure 1. This process was executed using a transesterification apparatus. The oil mixture was put into a round-bottom flask containing 500 g for each experiment, which was then set onto the transesterification apparatus. Applying the design of experiment (DOE) values indicated in Table 6, the oil mixture underwent preliminary heating on the transesterification apparatus to start the process. Calcium oxide was added to the methanol in the recommended amount. This amalgamation was agitated until the complete integration of the catalyst with the methanol resulted in a solution termed the "methoxide solution". Subsequently, the oil mixture that had been heated was filled with the methoxide solution. The transesterification apparatus speed was adjusted up to the required revolutions per minute. Each experiment lasted for 120 min to guarantee that the chemical reaction could take place. Upon the culmination of these 120 min, the transesterification process was deemed complete. After being taken off the hot plate, the solution inside the flask was allowed to cool to room temperature for a brief interval. Following this, following 24 h of inactivity, the solution was moved into a separating funnel. Upon the subsequent day, the

solution had separated into two distinct layers. Glycerol was present in the bottom layer, which comprised an unreacted catalyst and surplus methanol. In contrast, the upper layer consisted of biodiesel. Finally, the separating funnel was used to extract the glycerol and the biodiesel was retained for subsequent washing procedures.

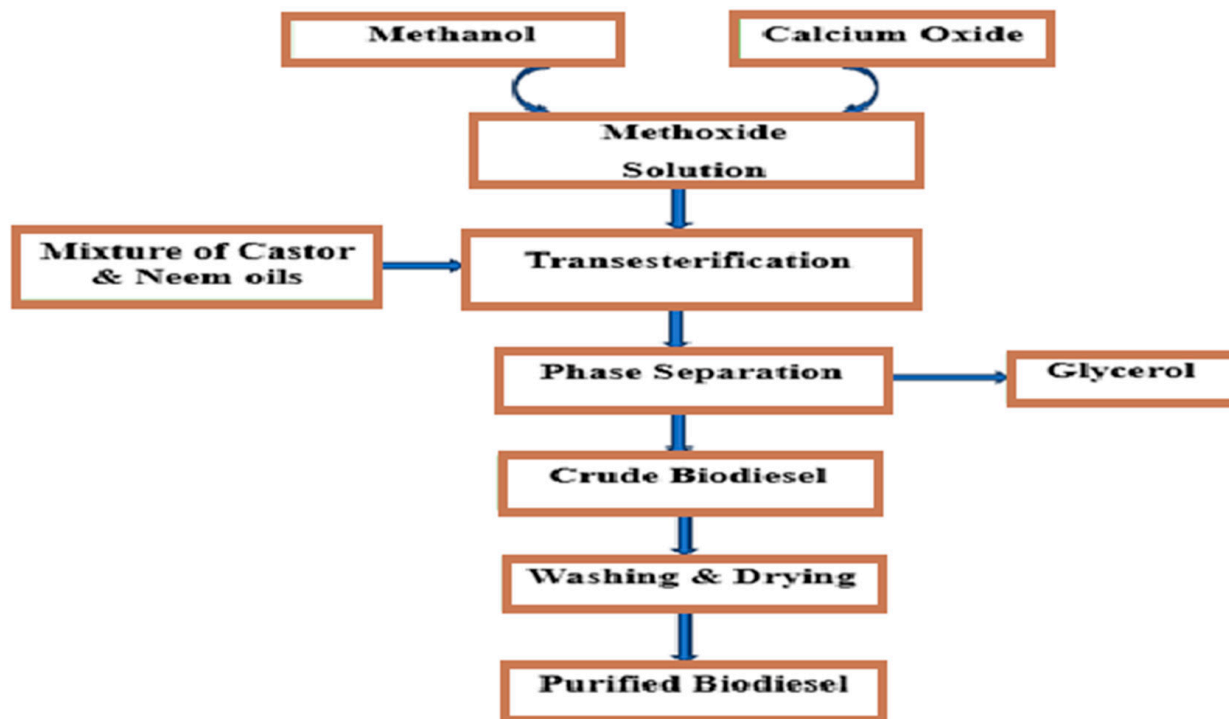


**Figure 1.** Biodiesel production steps.

In the biodiesel production process, a product known as crude biodiesel contains impurities, notably glycerol, unreacted methanol, and an excess of the catalyst. To eliminate these impurities, a washing procedure utilizing 20% distilled water was implemented. Initially, the 20% *v/v* oil of distilled water was heated and subsequently introduced into the crude biodiesel within the separating funnel. The blend of unrefined biodiesel and heated distilled water was vigorously agitated and then allowed to stand for a brief period. Following this, it was observed that the distilled water, along with the impurities, accumulated in the funnel's bottom for separation. The contaminants that had been separated from the funnel were present in this water layer. This process was repeated 3–4 times until a distinct layer of clear water was evident at the bottom of the separating funnel. The residual water present in the product was dried by introducing anhydrous sodium sulfate. Following the drying process with anhydrous sodium sulfate, filtration was performed. The desired biodiesel was the final product that was obtained after drying and filtering.

The biodiesel yield was determined by applying Equation (1).

$$\text{Biodiesel yield} = (\text{weight (g) of biodiesel}) / (\text{weight (g) of oil in the sample}) \times 100\% \quad (1)$$

#### 2.4. Gas Chromatography Analysis

Gas chromatography (GC) stands as a prevalent method utilized to analyze the mixture composition [31]. The GC analyzer (Shimadzu 2014) was employed to ascertain the FAME composition of the produced biodiesel. Operational parameters employed for evaluating the FAME composition are presented in Table 1. We used the capillary column for the separation in GC.

**Table 1.** Operating conditions for the composition of fatty acid methyl ester (FAME) in a gas chromatography (GC) test.

Sr /No.	Configurations	Details
1	Transporter gas	Nitrogen
2	Rate of flow	Fix rate
3	Temperature of injection	300 °C
4	Temperature of detector	300 °C
5	The kind of injection	Separate
6	The kind of detector	Ionization of flame injector
7	Volume of injection	1 micro liter
8	Column of capillary	(0.53 mm × 30 m, 0.5l m films)

### 2.5. Design of Experiment

The central composite design (CCD) was utilized as the experimental approach for the transesterification process of the castor and neem oil mixture. This design is advantageous for adjusting variables precisely, facilitating the achievement of ideal conditions while minimizing the number of required experimental trials [32]. A single response variable and three input factors were selected for the CCD in the transesterification process. A single response variable and three input factors were selected for the CCD in the esterification process, while a single response variable and four input factors were selected for the CCD in the transesterification process. The catalyst concentration, stirring speed, reaction process temperature, and methanol/oil mole ratio were the input parameters. The esterification process's acid value and the transesterification process's biodiesel yield were represented by the response variable. Table 2 provides a summary of the three input factors, along with their respective units and the range of values they encompassed in the experiments. Table 3 provides a summary of the four input variables, the corresponding units, and the range of values they encompassed during the trials.

**Table 2.** Experimental design for the esterification process.

Independent Factors	Units	−2 Level	−1 Level	0 Level
Methanol-to-oil molar ratio (A)	(mol/mol)	6	9	7.5
Catalyst conc. (B)	(w/w)	1	2.50	1.75
Temperature (C)	(°C)	50	60	55

**Table 3.** Experimental design for the transesterification process.

Independent Factors	Units	−2 Level	−1 Level	0 Level
Methanol-to-oil mole ratio (A)	(mol/mol)	6	12	9
Heterogeneous catalyst conc. (B)	(w/w)	1.5	3.50	2.5
Temperature (C)	(°C)	50	60	55
Stirring speed (D)	(rpm)	600	800	700

### 2.6. Statistical Analysis

The experiments were designed by the program used for the experimental data, Design Expert 7.0. During the design phase, the software was primarily concerned with determining the oil mixture's acid value and the biodiesel production as the response factor. To demonstrate how the response factor and the input factors are related, the quadratic polynomial equation was created. In order to forecast the yield as a dependent variable, Equation (2) was examined. Equation (2) was investigated in order to forecast

the yield as a dependent variable and input factors and to consider their interactions and interdependencies within the equation.

$$Y = \beta_0 + \sum_{i=1}^n \beta_i + \sum_{i=1}^n \beta_{ii} X_i^2 + \sum_{i=1}^{n-1} \sum_{j=i+1}^n \beta_{ij} X_{ij} \tag{2}$$

Y stands for the expected production of biodiesel,  $X_i$  is the input factor for  $i$ th; also, the different coefficients such as  $\beta_0$  (intercept),  $\beta_i$  (the first-order model’s coefficients),  $\beta_{ii}$  (coefficients for the quadratic model of each input factor), and  $\beta_{ij}$  (coefficients between different input factors) are utilized within the equation. The statistical significance of the independent variables’ values and their interactions was determined using an analysis of variance (ANOVA). ANOVA was used to consider experimental variation. Additionally, for the F-value and  $p$ -value, and to evaluate the independent variables’ statistical significance, their interactions, and the fit quality of the fitted model, an ANOVA was employed.

### 2.7. Determining the Properties of Biodiesel

The characteristics of generating biodiesel, encompassing density, kinematic viscosity, calorific value, flashpoint, cloud, pour point, acid value, and water content value, were assessed by the prescribed procedures outlined in the ASTM standards as mentioned in Table 4.

**Table 4.** Standard methods and testing apparatus for fuel properties.

Sr/No.	Properties	ASTM Methods	Testing Equipment
1	Density (kg/m <sup>3</sup> )	D-445	Gravity Meter
2	Kinematic Viscosity (mm <sup>2</sup> /s)	D-445	Cannon Viscometer
3	Calorific Value (MJ/kg)	OEM	Bomb Calorimeter
4	Acidic No. (mg KOH/g)	D-974	Titration
5	Flash Point (°C)	D-92	Open Cup Cleaveland
6	Pour Point (°C)	D-97	Pour Point Apparatus
7	Fire Point (°C)	D-92	Open Cup Cleaveland

## 3. Result and Discussion

### 3.1. Regression Model Equation

The oil’s experimental acid value, as detailed in Table 5, ranged from 8.3 to 4.9 mg of KOH/g oil. The experimental biodiesel yield, as detailed in Table 6, ranged from 35% to 93%. These coefficients were then applied to Equation (2). Equations (3) and (4) display the needed quadratic models as coded units.

$$AcidValue = +4.97 - 0.066 \times A - 0.23 \times B - 0.047 \times C - 0.025 \times A \times B - 0.037 \times A \times C - 0.037 \times B \times C + 1.11 \times A^2 + 0.74 \times B^2 + 0.21C^2 \tag{3}$$

$$Yield = +89.75 - 2.29 \times A + 3.29 \times B + 3.62 \times C + 1.71 \times D - 0.69 \times A \times B + 0.56 \times A \times C + 0.19 \times A \times D + 1.44 \times B \times C + 0.063 \times C \times D - 12.66 \times A^2 - 6.9B^2 - 6.16C^2 - 0.41D^2 \tag{4}$$

**Table 5.** Results of CCD for esterification process.

Exp.	Point Type	Methanol-to-Oil Mole Ratio (mol/mol) A	Catalyst Conc. (wt.%) B	Temperature (°C) C	Acid Value (mg of KOH/g Oil)
1	Fact	6:1	1.00	50	7.2
2	Fact	9:1	1.00	50	7.25

Table 5. Cont.

Exp.	Point Type	Methanol-to-Oil Mole Ratio (mol/mol) A	Catalyst Conc. (wt.%) B	Temperature (°C) C	Acid Value (mg of KOH/g Oil)
3	Fact	6:1	2.50	50	6.9
4	Fact	9:1	2.50	50	6.8
5	Fact	6:1	1.00	60	7.3
6	Fact	9:1	1.00	60	7.15
7	Fact	6:1	2.50	60	6.8
8	Fact	9:1	2.50	60	6.6
9	Axial	4.98:1	1.75	55	8.3
10	Axial	10.02:1	1.75	55	8.0
11	Axial	7.5:1	0.49	55	7.5
12	Axial	7.5:1	3.01	55	6.7
13	Axial	7.5:1	1.75	46.59	5.7
14	Axial	7.5:1	1.75	63.41	5.5
15	Center	7.5:1	1.75	55	4.9
16	Center	7.5:1	1.75	55	4.95
17	Center	7.5:1	1.75	55	5.0
18	Center	7.5:1	1.75	55	4.9
19	Center	7.5:1	1.75	55	5.05
20	Center	7.5:1	1.75	55	5.02

Table 6. Results of CCD for transesterification process.

Exp.	Point Type	Methanol/Oil Mole Ratio (mol/mol) A	Catalyst Conc. (wt.%) B	Temperature (°C) C	Agitation Speed (rpm) D	Biodiesel Yield (%)
1	Fact	6:1	1.50	50	600	60
2	Fact	12:1	1.50	50	600	55
3	Fact	6:1	3.50	50	600	63
4	Fact	12:1	3.50	50	600	56
5	Fact	6:1	1.50	60	600	64
6	Fact	12:1	1.50	60	600	60
7	Fact	6:1	3.50	60	600	73
8	Fact	12:1	3.50	60	600	68
9	Fact	6:1	1.50	50	800	62
10	Fact	12:1	1.50	50	800	58
11	Fact	6:1	3.50	50	800	66
12	Fact	12:1	3.50	50	800	58
13	Fact	6:1	1.50	60	800	66
14	Fact	12:1	1.50	60	800	65
15	Fact	6:1	3.50	60	800	75
16	Fact	12:1	3.50	60	800	70
17	Axial	3:1	2.50	55	700	43

Table 6. Cont.

Exp.	Point Type	Methanol/Oil Mole Ratio (mol/mol) A	Catalyst Conc. (wt.%) B	Temperature (°C) C	Agitation Speed (rpm) D	Biodiesel Yield (%)
18	Axial	15:1	2.50	55	700	35
19	Axial	9:1	0.50	55	700	52
20	Axial	9:1	4.50	55	700	72
21	Axial	9:1	2.50	45	700	59
22	Axial	9:1	2.50	65	700	71
23	Axial	9:1	2.50	55	500	83
24	Axial	9:1	2.50	55	900	93
25	Center	9:1	2.50	55	700	89
26	Center	9:1	2.50	55	700	91.5
27	Center	9:1	2.50	55	700	91
28	Center	9:1	2.50	55	700	88
29	Center	9:1	2.50	55	700	90.5
30	Center	9:1	2.50	55	700	88.5

Independent input factors selected for the esterification process were responsible for 98.83% of the variation in results, according to the model's correlation value ( $R^2$ ) of 0.9983. Similarly, independent input factors selected for the transesterification process were responsible for 98.06% of the variation in results, according to the model's correlation value ( $R^2$ ) of 0.9906. Ideally, a high degree of agreement between the experimental and predicted results is indicated by an  $R^2$  value of 1. The correlation between the predicted and experimental findings based on the constructed model was demonstrated in Figures 2 and 3.

Design-Expert® Software  
Acid Value

Color points by value of  
Acid Value:

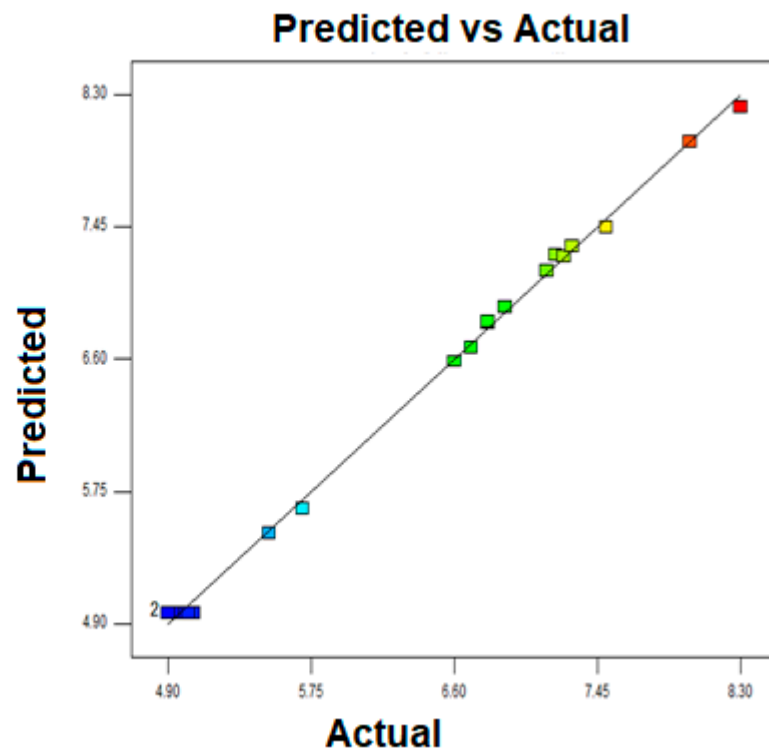
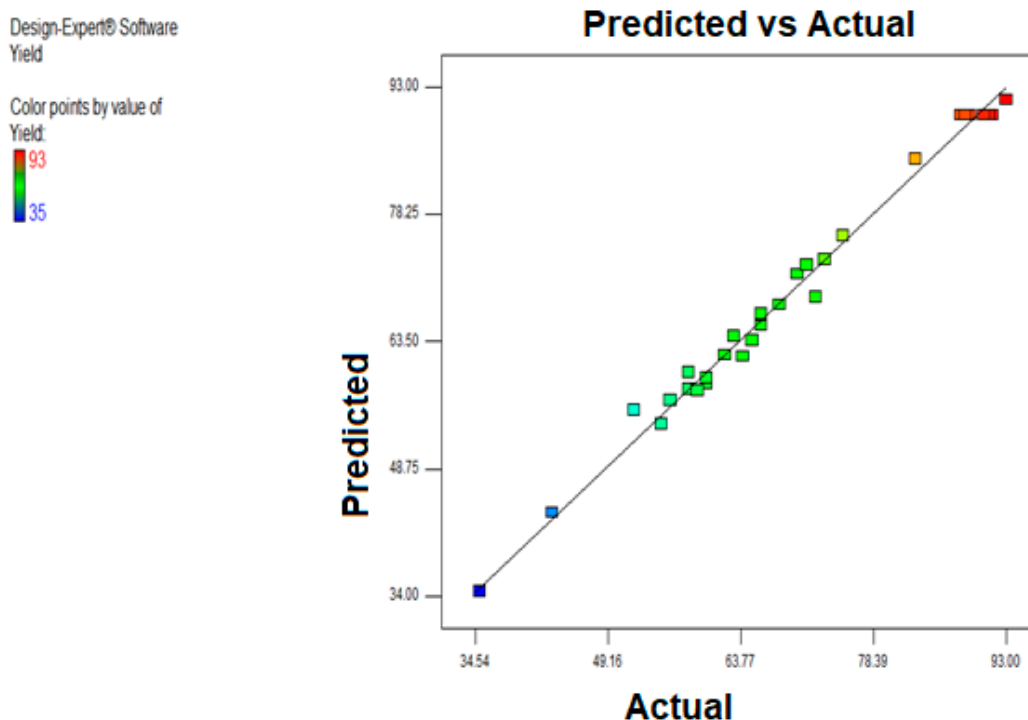


Figure 2. Predicted acid value versus actual acid value (mg of KOH/g oil).



**Figure 3.** Comparison of predicted and actual yields (%).

3.2. Statistical Analysis of Processes

3.2.1. Statistical Analysis of Esterification Process

Table 7 displays the results of the response surface quadratic model statistical analysis performed with ANOVA. The *p*-values and significance of each coefficient are shown in Table 7. The model’s importance was demonstrated by its Model F-value of 612.34, which indicated how unlikely it is at only 0.01% that such a large Model F-value could exist. On the other hand, values greater than 0.1000 suggested that the model terms are not significant. If the “Lack of Fit F-value” is 1.21, this indicates that, in comparison to pure error, the Lack of Fit is not statistically significant. The values of R-Squared, Adj R-Squared, Pred R-Squared, and Adeq Precision are given in Table 8. According to the computed R2 value of 0.9982, 99% of experimental data agree with the expected values of the model. The findings of the fitted model were reliable, as shown by the coefficient of variation of 1.04%.

**Table 7.** Analysis of variance (ANOVA) for response model.

Source	Sum of Squares	df	Mean Square	F-Value	<i>p</i> -Value Prob > F	
Model	24.349	9	2.705	612.34	<0.0001	Significant
A—Methanol/hybrid oil	0.060	1	0.060	13.56	0.0042	
B—Catalyst conc.	0.724	1	0.724	163.97	<0.0001	
C—Temperature	0.030	1	0.030	6.71	0.0269	
AB	0.005	1	0.005	1.13	0.3124	
AC	0.011	1	0.011	2.55	0.1416	
BC	0.011	1	0.011	2.55	0.1416	
A2	17.740	1	17.740	4015.35	<0.0001	
B2	7.855	1	7.855	1777.87	<0.0001	
C2	0.623	1	0.623	141.05	<0.0001	
Residual	0.044	10	0.004			

**Table 7.** *Cont.*

Source	Sum of Squares	df	Mean Square	F-Value	p-Value Prob > F	
Lack of Fit	0.024	5	0.005	1.21	0.4200	not significant
Pure error	0.020	5	0.004			
Cor total	24.393	19				

**Table 8.** Coefficient of regression analysis for esterification process.

C.V. %	R-Squared	Adj R-Squared	Pred R-Squared	Adeq Precision
1.01	0.9983	0.9967	0.9914	71.1599

### 3.2.2. Statistical Analysis of the Transesterification Process

Table 9 displayed the results of the response surface quadratic model statistical analysis performed with ANOVA. The *p*-values and significance of each coefficient are shown in Table 9. The model’s importance was demonstrated by its Model F-value of 113.9, which indicated how unlikely it is at only 0.01% that such a large “Model F-value” could exist. On the other hand, the model terms were not significant when values exceeded 0.100. If the “Lack of Fit F-value” was 2.47, this suggested that compared to the pure error, there was no statistically significant Lack of Fit. Table 10 provided the R-Squared, Adj R-Squared, Pred R-Squared, and Adeq Precision values. According to the computed R-squared value of 0.9906, 99% of experimental data agree with the expected values of the model. The findings of the fitted model were reliable, as shown by a coefficient of variation of 2.94%.

**Table 9.** Response model analysis of variance (ANOVA).

Source	Squares Sum	df	Square Mean	F-Value	p-Value Prob > F	
Model	6504.45	14	464.60	113.09	<0.0001	Significant
A—Methanol/oil	126.04	1	126.04	30.68	<0.0001	
B—Catalyst concentration	260.04	1	260.04	63.30	<0.0001	
C—Temperature	315.38	1	315.38	76.76	<0.0001	
D—Steering speed	70.04	1	70.04	17.05	0.0009	
AB	7.56	1	7.56	1.84	0.1949	
AC	5.07	1	5.07	1.23	0.2844	
AD	0.57	1	0.57	0.14	0.7165	
BC	33.06	1	33.06	8.05	0.0125	
BD	0.56	1	0.56	0.14	0.7165	
CD	0.06	1	0.06	0.02	0.9035	
A2	4393.53	1	4393.53	1069.42	<0.0001	
B2	1308.24	1	1308.24	318.44	<0.0001	
C2	1039.53	1	1039.53	253.03	<0.0001	
D2	4.53	1	4.53	1.10	0.3105	
Residual	61.63	15	4.11			
Lack of Fit	51.25	10	5.13	2.47	0.1651	not significant
Pure error	10.38	5	2.08			
Cor total	6566.08	29				

**Table 10.** Coefficient of regression analysis for transesterification process.

C.V. %	R-Squared	Pred R-Squared	Adj R-Squared	Adeq Precision
2.94	0.9906	0.9528	0.9819	29.770

### 3.3. Interactions Among the Process Variables

#### 3.3.1. Interactions Among the Esterification Process Variables

Figure 4 presents 3D surface graphs to explore how multiple process variables collectively affect the acid value rather than focusing on individual variables. Figure 4a presents a 3D surface response depicting the combined influence of varying methanol-to-oil molar ratios (between 6 and 19 mol/mol) and different catalyst concentrations (between 1.5 and 2.5 wt.%) on acid value while maintaining temperature (55 °C). Notably, when catalyst concentration increased from 1.75 wt.% to 2.5 wt.%, and the methanol-to-oil ratio increased from 7.5 mol/mol to 9 mol/mol, the acid value significantly increased from 4.9 to 6.8.

The methanol greatly influences the esterification process in regard to the oil ratio. At first, the amount of free fatty acids (FFA) did not decrease when the molar ratio was increased to 6:1. This is explained by the fact that esters are usually produced when one mole of FFA interacts with one mole of methanol. To improve the ester formation rate and move the equilibrium in the direction of the intended forward reaction, a significant quantity of methanol is required. While this approach can lead to the production of water as a by-product, it has the drawback of potentially reversing the reaction, decreasing the forward reaction rate and prolonging the separation process [33].

Based on the findings, it is clear that sulfuric acid serves as an effective catalyst for acid esterification. Nevertheless, the reduction in free fatty acids (FFA) is only slightly affected by raising the catalyst's concentration. This limited effect may be attributed to the oil sample's elevated water content and the water produced throughout the esterification procedure. Clear increases in the number of accessible acid moieties were observed when the catalyst content rose to 1.75 weight percent. The conversion ratio dropped as catalyst concentration rose above 1.75 weight percent. Most likely, this was because of the growing negative effects brought on by the rising acidity, a greater quantity of catalysts in the reaction system, and the molecules of the product being adsorbed by an excessive number of catalysts, which can cause the mass transfer resistance to increase. Consequently, a 1.75 weight percent worked best in this esterification reaction [34].

Figure 4b presents a 3D surface response depicting the combined influence of different methanol-to-oil molar ratios (between 6 and 9 mol/mol) and temperature (between 50 °C and 60 °C) on acid value while maintaining catalyst concentration (1.75 wt.%). The figure clearly demonstrates that the acid value decreased from 5.5 to 4.9 when the temperature was raised between 50 °C and 55 °C at a molar ratio of 7.50 methanol-to-oil. The reason for this is that a moderate temperature increase enhances the oil's solubility in methanol and reduces the oil mixture's percentage of free fatty acids (%FFA). This suggests that temperatures both below and above 55 °C have a negative impact on decreasing the FFA content [35].

Figure 4c presents a 3D surface response depicting the combined influence of varying catalyst concentrations (between 1.5 and 2.5 wt.%) and temperatures (between 50 °C and 60 °C) on the acid value while maintaining the molar ratio of 7.50 methanol-to-oil. When the temperature was increased from 50 °C to 55 °C and the catalyst concentration increased from 1 wt.% to 1.75 wt.%, the acid value lowered considerably from 6.5 to 5.02.

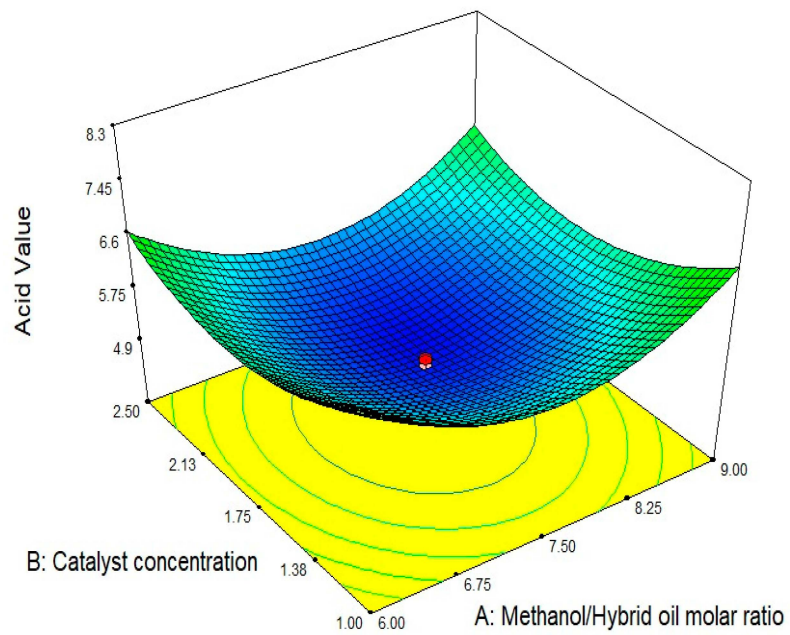
Design-Expert® Software

Acid Value



X1 = A: Methanol/Hybrid oil molar ratio  
X2 = B: Catalyst concentration

Actual Factor  
C: Temperature = 55.00



(a)

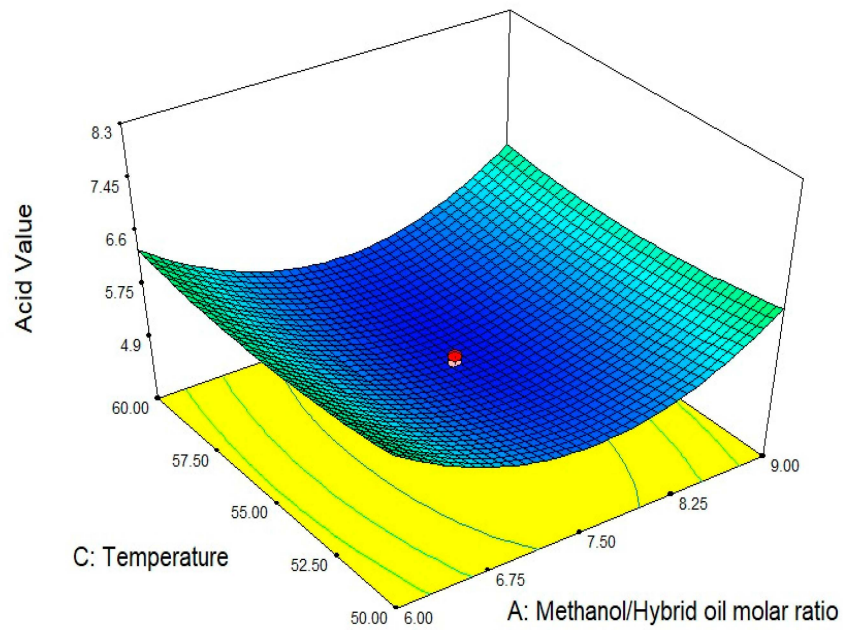
Design-Expert® Software

Acid Value



X1 = A: Methanol/Hybrid oil molar ratio  
X2 = C: Temperature

Actual Factor  
B: Catalyst concentration = 1.75



(b)

Figure 4. Cont.

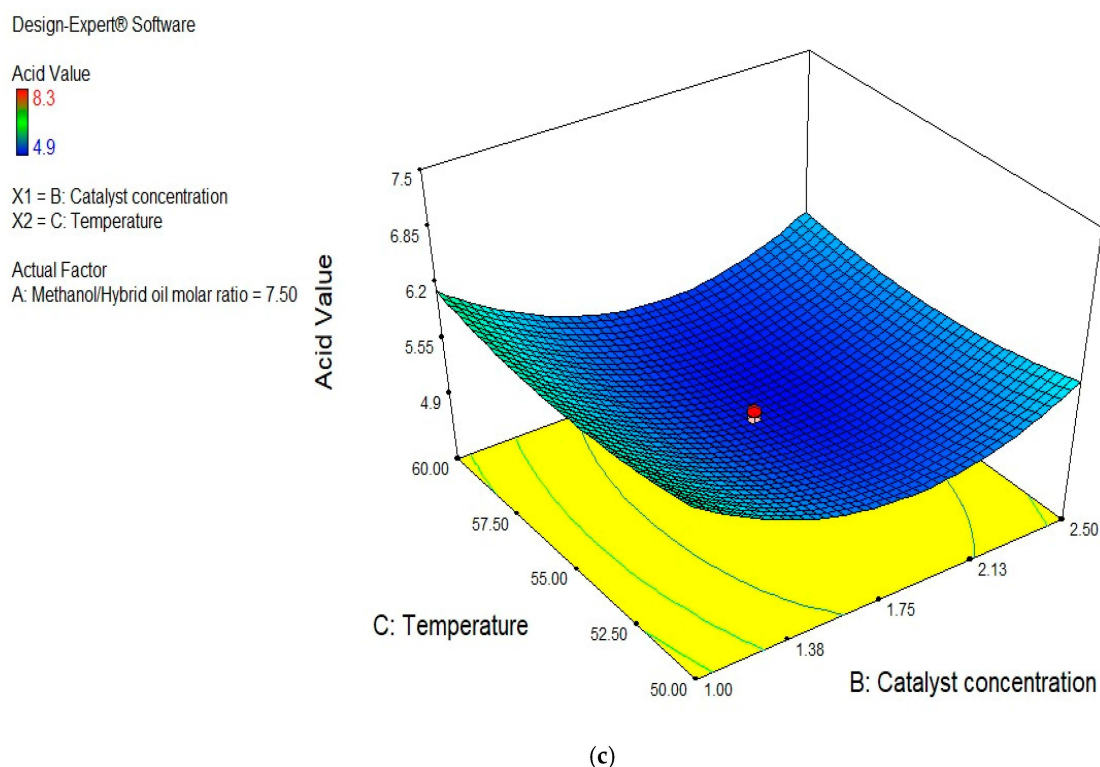


**Figure 4.** (a) Effect of methanol-to-oil molar ratio and catalyst concentration on acid value. (b) Effect of methanol-to-oil molar ratio and temperature on acid value. (c) Effect of catalyst concentration and temperature on acid value.

### 3.3.2. Interactions Between the Transesterification Process Variables

Figure 5 presents 3D surface graphs to explore how multiple process variables collectively affect the production of biodiesel rather than focusing on individual variables. Figure 5a illustrates the interplay between methanol/oil molar ratios (between 6 and 12 mol/mol) and catalyst concentrations (between 1.5 and 2.5 wt.%) on biodiesel yield within a fixed temperature of 55 °C and stirring speed of 700 rpm. Notably, biodiesel yield increased significantly, going from 65% to 92%, as the methanol/oil mole ratio rose from 6 to 9, and the concentration of the catalyst rose between 1.5 wt.% to 2.5 wt.%. When the methanol/oil mole ratio expanded from 9 to 10.5, coupled with a catalyst concentration that rose from 2.5 wt.% to 3.0 wt.%, the biodiesel production dropped from 92% to 77%. Also, when the methanol/oil mole ratio expanded from 10.5 to 12, coupled with a catalyst concentration that rose from between 3.0 wt.% to 3.5 wt.%, the biodiesel production dropped from 77% to 63%.

When utilizing a concentration of catalyst of 2.5 wt.% and methanol/oil mole ratio of 9:1, a greater biodiesel yield was obtained [36]. When we exceeded the optimal range for the methanol/oil mole ratio, emulsion formation made the process of separating biodiesel from glycerol more complex, and the overall cost increased. Furthermore, the reaction mixture was diluted, and the catalyst's efficiency was decreased due to an excess of methanol [37,38].

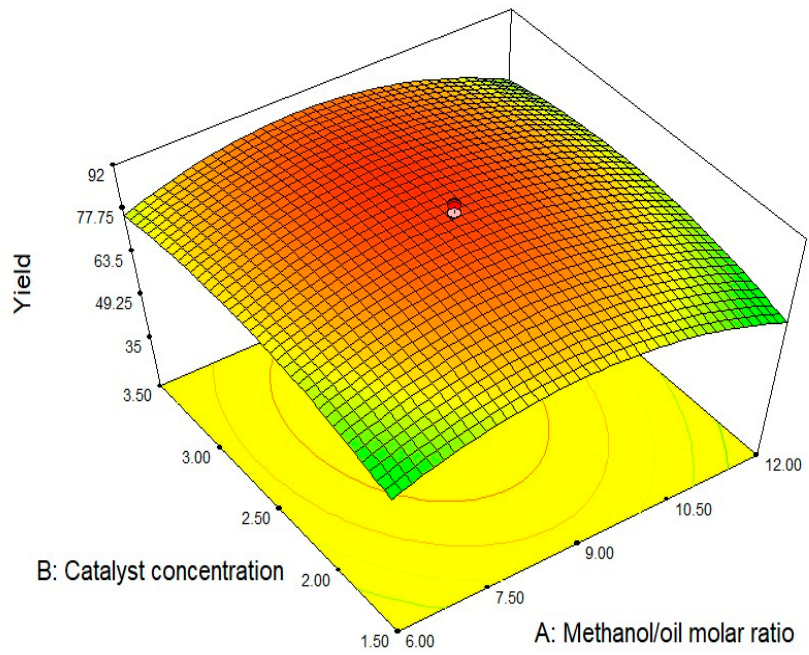
It was found that low catalyst concentrations were found to either leave the chemical reaction incomplete or to cause a minimal yield of biodiesel. However, as we increased the catalyst concentration up to the optimum value, the biodiesel yields improved [39]. Conversely, when the catalyst concentration exceeded the optimum value, the soap and glycerol content increased, causing the production of biodiesel to decline. Reactant viscosity increased as a result of increasing catalyst concentration during the chemical reaction, which eventually decreased the yield of biodiesel [40].

Design-Expert® Software



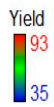
X1 = A: Methanol/oil molar ratio  
X2 = B: Catalyst concentration

Actual Factors  
C: Temperature = 55.00  
D: Stirring speed = 700.00



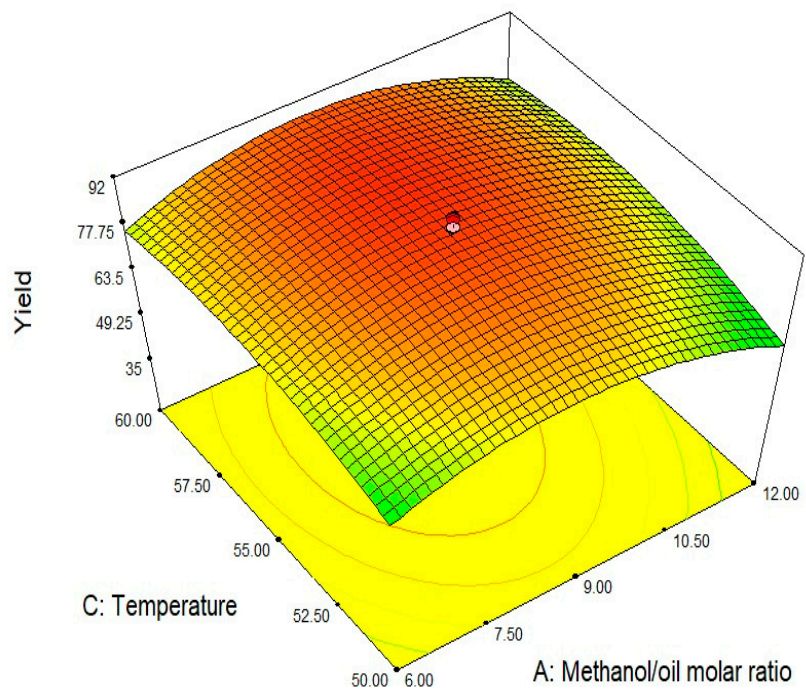
(a)

Design-Expert® Software



X1 = A: Methanol/oil molar ratio  
X2 = C: Temperature

Actual Factors  
B: Catalyst concentration = 2.50  
D: Stirring speed = 700.00



(b)

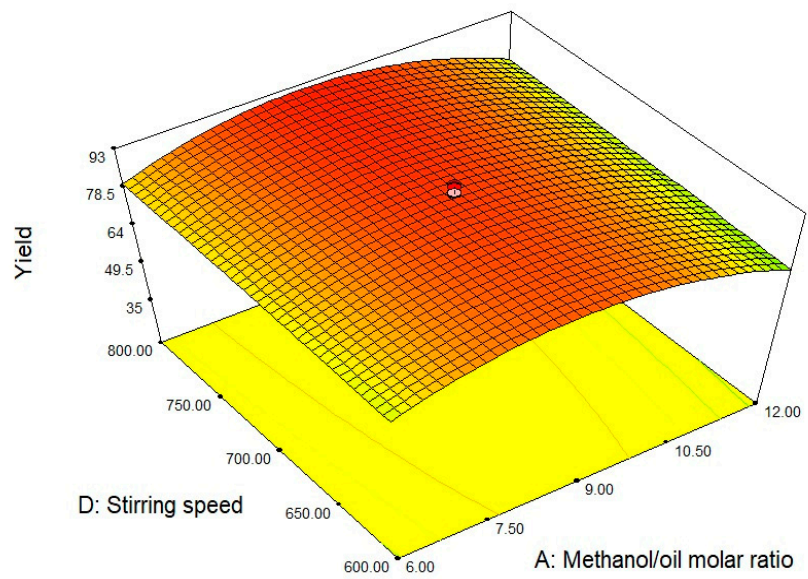
Figure 5. Cont.

Design-Expert® Software



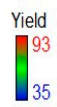
X1 = A: Methanol/oil molar ratio  
X2 = D: Stirring speed

Actual Factors  
B: Catalyst concentration = 2.50  
C: Temperature = 55.00



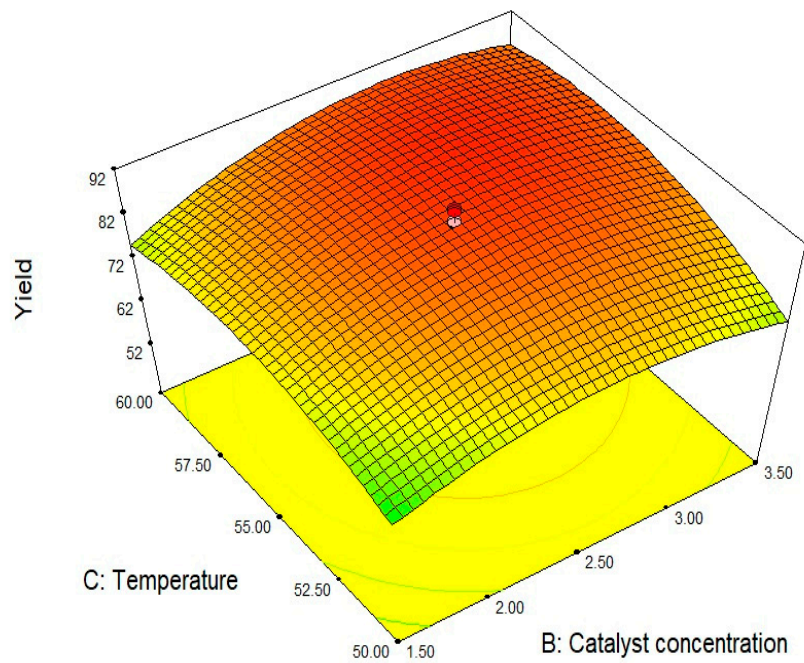
(c)

Design-Expert® Software



X1 = B: Catalyst concentration  
X2 = C: Temperature

Actual Factors  
A: Methanol/oil molar ratio = 9.00  
D: Stirring speed = 700.00



(d)

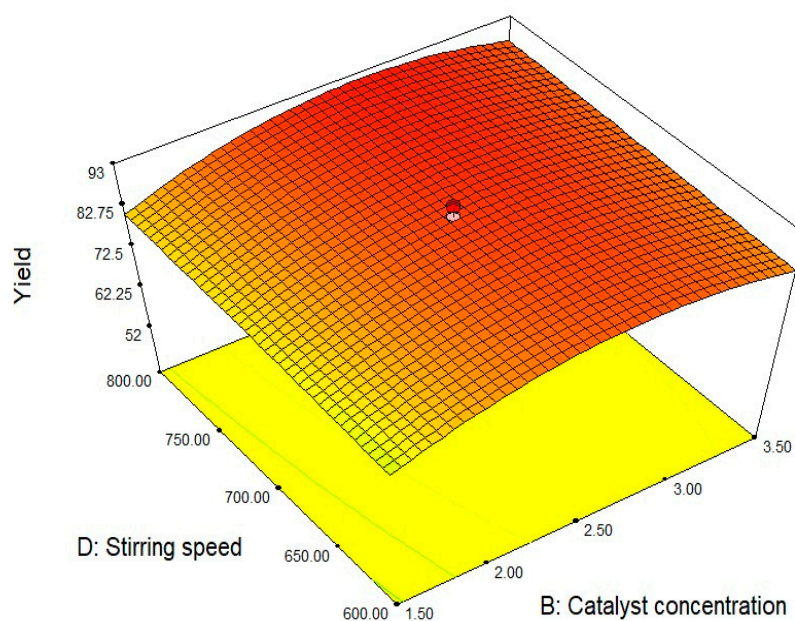
Figure 5. Cont.

Design-Expert® Software



X1 = B: Catalyst concentration  
X2 = D: Stirring speed

Actual Factors  
A: Methanol/oil molar ratio = 9.00  
C: Temperature = 55.00



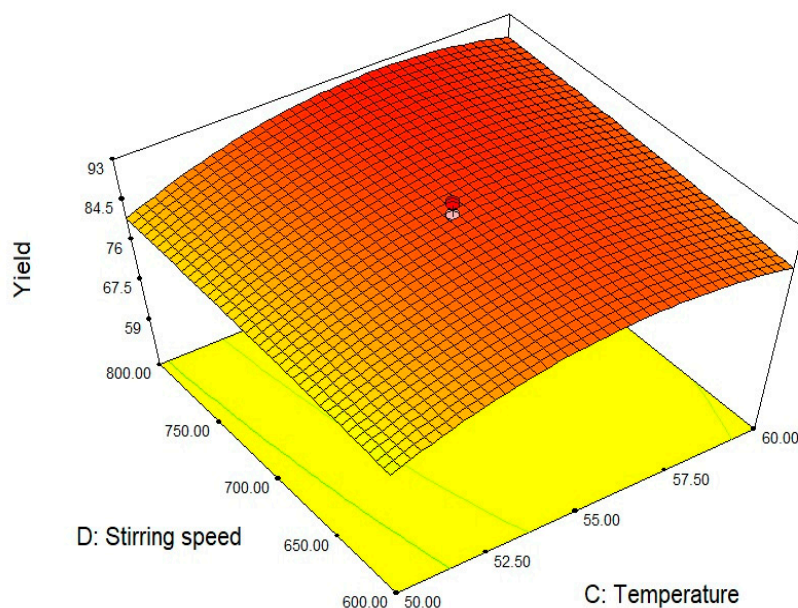
(e)

Design-Expert® Software



X1 = C: Temperature  
X2 = D: Stirring speed

Actual Factors  
A: Methanol/oil molar ratio = 9.00  
B: Catalyst concentration = 2.50



(f)

**Figure 5.** (a) Impact of methanol/oil mole ratio and concentration of catalyst on yield of biodiesel. (b) Impact of methanol/oil mole ratio and temperature on yield of biodiesel. (c) Impact of methanol-to-oil molar ratio and stirring speed on yield of biodiesel. (d) Impact of concentration of catalyst and temperature on yield of biodiesel. (e) Impact of concentration of catalyst and stirring speed on biodiesel yield. (f) Effect of temperature and stirring speed on yield of biodiesel.

In Figure 5b, the 3D surface response illustrated the combined impact of different methanol/oil mole ratios (from 6 to 12 mol/mol) and temperatures (between 50 and 60 °C) on biodiesel yield while keeping catalyst concentration fixed at 2.50 wt.% and keeping the stirring speed at 700 rpm all the while. The figure clearly demonstrated that the biodiesel yield increased significantly, rising from 58% to 90%, as methanol/oil increased between 6 and 9, and the temperature rose between 50 ° and 60 °C. Furthermore, elevating the

temperature to its optimal value caused the pore size to increase, crystal growth, and an increased porosity of the catalyst, ultimately enhancing the yield of biodiesel.

Figure 5c presents a 3D surface response depicting the resultant effect of different methanol/oil mole ratios (between 6 and 12 mol/mol) and stirring speeds (between 600 and 800 rpm) on biodiesel yield while maintaining a constant catalyst concentration (2.50 wt.%) and temperature (55 °C). The figure clearly illustrates that when the pace of stirring accelerated from 600 to 800 rpm, especially when the methanol/oil mole ratio was 9:1, the biodiesel yield saw a noticeable enhancement, rising from 85% to 90.5%. This improvement can be attributed to the expansion of the reaction area for both the oil and methanol phases when the stirring speed was increased. Additionally, the acceleration in stirring speed leads to a more rapid collision between oil and methanol molecules with the catalyst's active surface sites, which increases the possibility of biodiesel production.

In Figure 5d, a 3D surface response exhibits the collective effect of varying different catalyst concentrations (between 1.5 and 3.5 wt.%) and temperatures (between 50 and 60 °C) on biodiesel output while continuing to stir at a steady 700 rpm and keeping the methanol/oil mole ratio constant at 9 mol/mol. The figure clearly illustrates a significant improvement in the yield of biodiesel from 69% to 90.5% when we elevated both the catalyst concentration from 1.50 to 2.50 and temperature between 50 ° and 55 °C.

In Figure 5e, a 3D surface response graph demonstrates the joint influence of varying different catalyst concentrations (between 1.5 and 3.5 wt.%) and stirring speeds (between 600 and 800 rpm) on biodiesel yield. This is carried out while keeping the temperature (55 °C) and the methanol/oil mole ratio (9 mol/mol) constant. The figure distinctly reveals that as we increased the stirring speed from 600 to 800 rpm while keeping the catalyst concentration fixed at 2.5 wt.%, the biodiesel yield experienced a discernible boost, climbing from 78% to 89.5%.

Figure 5f displayed a 3D surface response plot that illustrated how the simultaneous variation of temperature (between 50 and 60 °C) and stirring speed (between 600 and 800 rpm) affects the biodiesel yield. This analysis maintains a constant methanol/oil mole ratio (9 mol/mol) and a fixed concentration of catalyst (2.5 wt.%). The figure conspicuously highlights a rise in the production of biodiesel, moving from 81% to 88.3%, while the speed of stirring was increased from 600 to 800 rpm while holding the temperature constant at 55 °C.

### 3.4. Composition and Physicochemical Properties of Biodiesel

The FAME composition changed depending on the biodiesel source. Saturated acids like palmitic acid, lauric acid, and stearic acid account for 8.3%, 0.64%, and 8.4% of the composition, respectively. However, unsaturated acids, including oleic acid, linoleic acid, and ricinoleic acid, make up 28.2%, 4.5%, and 49.4% of the mixture, respectively. Following the two-step production process, the resulting methyl ester underwent detailed analysis to assess its physicochemical properties. Physicochemical parameters such as density, acid value, pour point, cloud point, kinematic viscosity, flash point, and calorific value met the standards outlined in ASTM D6751. The specific physicochemical attributes of the methyl ester can be found in Table 11.

**Table 11.** Properties of fuels and comparison with the ASTM standard values.

Sr/No.	Properties	Diesel Fuel	Biodiesel 100	B10	B20	B30	ASTM D6751 [41]	EN 14214 [42]
1	Density (kg/m <sup>3</sup> )	812	903	817	826	835	880	860–900
2	Kinematic viscosity (mm <sup>2</sup> /s)	1.72	3.14	1.85	2.01	2.13	1.9–6	3.5–5
3	Calorific value (MJ/kg)	45.5	38.8	44.6	43.9	43.2	-	35

Table 11. Cont.

Sr/No.	Properties	Diesel Fuel	Biodiesel 100	B10	B20	B30	ASTM D6751 [41]	EN 14214 [42]
4	Acidic number (mg KOH/g)	0.07	0.32	0.107	0.129	0.151	Max0.5	Max0.5
5	Flash point (°C)	77	190	81.6	89.3	97.1	Min130	Min130
6	Pour point (°C)	−12	−8	−11.3	−10.8	−10.3	-	-
7	Cloud point (°C)	−9	−6	−8.2	−7.8	−7.3	-	-
8	Fire point (°C)	83	197	85	91	98	-	-

#### 4. Conclusions

This study examined the utilization of nonedible oils; in particular, a combination of castor and neem oils. This combination offered a workable method for producing biodiesel that can be used as an alternative blended fuel source. A central composite design (CCD) was used to optimize production process parameters in esterification and transesterification processes. For the esterification step, a methanol-to-oil molar ratio of 7.5:1, 1.75 wt.% of H<sub>2</sub>SO<sub>4</sub>, and a temperature of 55 °C were optimal. In the transesterification step, optimized conditions included a methanol-to-oil molar ratio of 9:1, a 2.50 wt.% of calcium oxide, a temperature of 55 °C, and a stirring speed of 900 rpm, resulting in a 93% yield of methyl ester. Different properties of the produced biodiesel were examined and found within the limits of the standards ASTM D6751 and EN 14214. Hence, the mixture of castor and neem oil biodiesel can be used as an alternative blended fuel source for diesel engines.

**Author Contributions:** Conceptualization, M.A. and M.J.; methodology, H.A.; software, A.A. and F.B.A.; formal analysis, M.A. and F.B.A.; investigation, A.A.Q. and F.B.A.; resources, A.A.Q., H.L.A. and M.U.K.; data curation, H.A. and M.A. writing—original draft preparation, H.A.; writing—review and editing, H.A., M.J., M.A.K., F.B.A., H.L.A., M.U.A.K. and M.U.K.; visualization, A.A. and M.U.A.K.; supervision, M.J., H.H.M. and M.A.K.; project administration, M.J., H.H.M. and M.A.K.; funding acquisition, M.J. and M.A.K. All authors have read and agreed to the published version of the manuscript.

**Funding:** This research received no external funding.

**Data Availability Statement:** The data presented in this study are available on request from the corresponding author.

**Acknowledgments:** The authors would like to acknowledge the Institute of Chemical Sciences (ICS) and the Department of Mechanical Engineering, Faculty of Engineering and Technology at Bahauddin Zakariya University Multan, for providing the lab facilities needed to conduct this experimental work.

**Conflicts of Interest:** The authors declare no conflict of interest.

#### References

- Zhang, S.; Pan, H.; Huang, J.; Li, Y.; Zhang, H. A highly effective biomass-derived solid acid catalyst for biodiesel synthesis through esterification. *Front. Chem.* **2022**, *10*, 882235. [[CrossRef](#)] [[PubMed](#)]
- Liu, Y.; Liu, X.; Li, M.; Meng, Y.; Li, J.; Zhang, Z.; Zhang, H. Recyclable Zr/Hf-containing acid-base bifunctional catalysts for hydrogen transfer upgrading of biofurans: A review. *Front. Chem.* **2021**, *9*, 812331. [[CrossRef](#)] [[PubMed](#)]
- Ong, H.C.; Tiong, Y.W.; Goh, B.H.H.; Gan, Y.Y.; Mofijur, M.; Fattah, I.R.; Chong, C.T.; Alam, M.A.; Lee, H.V.; Silitonga, A.S. Recent advances in biodiesel production from agricultural products and microalgae using ionic liquids: Opportunities and challenges. *Energy Convers. Manag.* **2021**, *228*, 113647. [[CrossRef](#)]
- Basumatary, S.; Nath, B.; Kalita, P. Application of agro-waste derived materials as heterogeneous base catalysts for biodiesel synthesis. *J. Renew. Sustain. Energy* **2018**, *10*, 043105. [[CrossRef](#)]
- Atabani, A.E.; Silitonga, A.S.; Badruddin, I.A.; Mahlia, T.; Masjuki, H.; Mekhilef, S. A comprehensive review on biodiesel as an alternative energy resource and its characteristics. *Renew. Sustain. Energy Rev.* **2012**, *16*, 2070–2093. [[CrossRef](#)]

6. Karmakar, R.; Kundu, K.; Rajor, A. Fuel properties and emission characteristics of biodiesel produced from unused algae grown in India. *Pet. Sci.* **2018**, *15*, 385–395. [[CrossRef](#)]
7. Gumus, M.; Kasifoglu, S. Performance and emission evaluation of a compression ignition engine using a biodiesel (apricot seed kernel oil methyl ester) and its blends with diesel fuel. *Biomass Bioenergy* **2010**, *34*, 134–139. [[CrossRef](#)]
8. Waseem, H.H.; El Zerey-Belaskri, A.; Nadeem, F.; Yaqoob, I. The downside of biodiesel fuel—A review. *Int. J. Chem. Biochem. Sci.* **2016**, *9*, 97–106.
9. Silitonga, A.; Masjuki, H.; Mahlia, T.; Ong, H.; Chong, W.; Boosroh, M. Overview properties of biodiesel diesel blends from edible and non-edible feedstock. *Renew. Sustain. Energy Rev.* **2013**, *22*, 346–360. [[CrossRef](#)]
10. Veljković, V.B.; Biberdžić, M.O.; Banković-Ilić, I.B.; Djalović, I.G.; Tasić, M.B.; Nježić, Z.B.; Stamenković, O.S. Biodiesel production from corn oil: A review. *Renew. Sustain. Energy Rev.* **2018**, *91*, 531–548. [[CrossRef](#)]
11. Zhong, W.; Huang, X.; Yan, F.; Pachiannan, T.; Wang, J.; He, Z.; Wang, Q. A Comparative Study of first and second generation Biodiesel Blends under Quaternary Injection Strategies for Enhanced Engine Performance and Reduced Emissions. *Process Saf. Environ. Prot.* **2024**, *191*, 605–615.
12. Mishra, V.K.; Goswami, R. A review of production, properties and advantages of biodiesel. *Biofuels* **2018**, *9*, 273–289. [[CrossRef](#)]
13. Martínez, G.; Sánchez, N.; Encinar, J.; González, J. Fuel properties of biodiesel from vegetable oils and oil mixtures. Influence of methyl esters distribution. *Biomass Bioenergy* **2014**, *63*, 22–32. [[CrossRef](#)]
14. Sharma, Y.; Singh, B. A hybrid feedstock for a very efficient preparation of biodiesel. *Fuel Process. Technol.* **2010**, *91*, 1267–1273. [[CrossRef](#)]
15. Dwivedi, G.; Sharma, M. Potential and limitation of straight vegetable oils as engine fuel—An Indian perspective. *Renew. Sustain. Energy Rev.* **2014**, *33*, 316–322. [[CrossRef](#)]
16. Wancura, J.H.; Rosset, D.V.; Brondani, M.; Mazutti, M.A.; Oliveira, J.V.; Tres, M.V.; Jahn, S.L. Soluble lipase-catalyzed synthesis of methyl esters using a blend of edible and nonedible raw materials. *Bioprocess Biosyst. Eng.* **2018**, *41*, 1185–1193. [[CrossRef](#)]
17. Falowo, O.A.; Oloko-Oba, M.I.; Betiku, E. Biodiesel production intensification via microwave irradiation-assisted transesterification of oil blend using nanoparticles from elephant-ear tree pod husk as a base heterogeneous catalyst. *Chem. Eng. Process. -Process Intensif.* **2019**, *140*, 157–170. [[CrossRef](#)]
18. Sharma, V.; Duraisamy, G. Production and characterization of bio-mix fuel produced from a ternary and quaternary mixture of raw oil feedstock. *J. Clean. Prod.* **2019**, *221*, 271–285. [[CrossRef](#)]
19. Adepoju, T. Optimization processes of biodiesel production from pig and neem (*Azadirachta indica* a. Juss) seeds blend oil using alternative catalysts from waste biomass. *Ind. Crops Prod.* **2020**, *149*, 112334. [[CrossRef](#)]
20. Mujtaba, M.; Masjuki, H.; Kalam, M.; Ong, H.C.; Gul, M.; Farooq, M.; Soudagar, M.E.M.; Ahmed, W.; Harith, M.; Yusoff, M. Ultrasound-assisted process optimization and tribological characteristics of biodiesel from palm-sesame oil via response surface methodology and extreme learning machine-Cuckoo search. *Renew. Energy* **2020**, *158*, 202–214. [[CrossRef](#)]
21. Niju, S.; Vishnupriya, G.; Balajii, M. Process optimization of Calophyllum inophyllum-waste cooking oil mixture for biodiesel production using Donax deltooides shells as heterogeneous catalyst. *Sustain. Environ. Res.* **2019**, *29*, 18. [[CrossRef](#)]
22. Kumar, D.; Das, T.; Giri, B.S.; Rene, E.R.; Verma, B. Biodiesel production from hybrid non-edible oil using bio-support beads immobilized with lipase from *Pseudomonas cepacia*. *Fuel* **2019**, *255*, 115801. [[CrossRef](#)]
23. Fadhil, A.B.; Nayyef, A.W.; Sedeeq, S.H. Valorization of mixed radish seed oil and *Prunus armeniaca* L. oil as a promising feedstock for biodiesel production: Evaluation and analysis of biodiesels. *Asia-Pac. J. Chem. Eng.* **2020**, *15*, e2390. [[CrossRef](#)]
24. Bhatia, S.K.; Bhatia, R.K.; Jeon, J.-M.; Pugazhendhi, A.; Awasthi, M.K.; Kumar, D.; Kumar, G.; Yoon, J.-J.; Yang, Y.-H. An overview on advancements in biobased transesterification methods for biodiesel production: Oil resources, extraction, biocatalysts, and process intensification technologies. *Fuel* **2021**, *285*, 119117. [[CrossRef](#)]
25. Tariq, M.; Ali, S.; Khalid, N. Activity of homogeneous and heterogeneous catalysts, spectroscopic and chromatographic characterization of biodiesel: A review. *Renew. Sustain. Energy Rev.* **2012**, *16*, 6303–6316. [[CrossRef](#)]
26. Su, F.; Guo, Y. Advancements in solid acid catalysts for biodiesel production. *Green Chem.* **2014**, *16*, 2934–2957. [[CrossRef](#)]
27. Orege, J.I.; Oderinde, O.; Kifle, G.A.; Ibikunle, A.A.; Raheem, S.A.; Ejeromedoghene, O.; Okeke, E.S.; Olukowi, O.M.; Orege, O.B.; Fagbohun, E.O. Recent advances in heterogeneous catalysis for green biodiesel production by transesterification. *Energy Convers. Manag.* **2022**, *258*, 115406. [[CrossRef](#)]
28. Mathers, C.D.; Ezzati, M.; Lopez, A.D. Measuring the burden of neglected tropical diseases: The global burden of disease framework. *PLoS Neglected Trop. Dis.* **2007**, *1*, e114. [[CrossRef](#)]
29. Brahma, S.; Basumatary, B.; Basumatary, S.F.; Das, B.; Brahma, S.; Rokhum, S.L.; Basumatary, S. Biodiesel production from quinary oil mixture using highly efficient *Musa chinensis* based heterogeneous catalyst. *Fuel* **2023**, *336*, 127150. [[CrossRef](#)]
30. Samuel, O.D.; Emajuwa, J.; Kaveh, M.; Emagbetere, E.; Abam, F.; Elumalai, P.; Enweremadu, C.C.; Reddy, P.S.; Eseoghene, I.D.; Mustafa, A. Neem-castor seed oil esterification modelling: Comparison of RSM and ANFIS. *Mater. Today Proc.* **2023**. [[CrossRef](#)]
31. Ostovan, A.; Ghaedi, M.; Arabi, M.; Yang, Q.; Li, J.; Chen, L. Hydrophilic multitemplate molecularly imprinted biopolymers based on a green synthesis strategy for determination of B-family vitamins. *ACS Appl. Mater. Interfaces* **2018**, *10*, 4140–4150. [[CrossRef](#)] [[PubMed](#)]
32. Arabi, M.; Ghaedi, M.; Ostovan, A. Development of dummy molecularly imprinted based on functionalized silica nanoparticles for determination of acrylamide in processed food by matrix solid phase dispersion. *Food Chem.* **2016**, *210*, 78–84. [[CrossRef](#)] [[PubMed](#)]

33. Azhari, F.M.; Yunus, R.; Ghazi, T.M.; Yaw, T. Reduction of free fatty acids in crude jatropha curcas oil via an esterification process. *Int. J. Eng. Technol.* **2008**, *5*, 92–98.
34. Halder, S.; Dhawane, S.H.; Kumar, T.; Halder, G. Acid-catalyzed esterification of castor (*Ricinus communis*) oil: Optimization through a central composite design approach. *Biofuels* **2015**, *6*, 191–201. [[CrossRef](#)]
35. Ajala, E.; Aberuagba, F.; Olaniyan, A.; Ajala, M.; Sunmonu, M. Optimization of a two stage process for biodiesel production from shea butter using response surface methodology. *Egypt. J. Pet.* **2017**, *26*, 943–955. [[CrossRef](#)]
36. Charoenchaitrakool, M.; Thienmethangkoon, J. Statistical optimization for biodiesel production from waste frying oil through two-step catalyzed process. *Fuel Process. Technol.* **2011**, *92*, 112–118. [[CrossRef](#)]
37. Fadhil, A.B.; Ahmed, A.I. Production and evaluation of biodiesel from mixed castor oil and waste chicken oil. *Energy Sources Part A Recovery Util. Environ. Eff.* **2016**, *38*, 2140–2147. [[CrossRef](#)]
38. Al-Hamamre, Z.; Yamin, J. Parametric study of the alkali catalyzed transesterification of waste frying oil for Biodiesel production. *Energy Convers. Manag.* **2014**, *79*, 246–254. [[CrossRef](#)]
39. Roschat, W.; Siritanon, T.; Yoosuk, B.; Promarak, V. Rice husk-derived sodium silicate as a highly efficient and low-cost basic heterogeneous catalyst for biodiesel production. *Energy Convers. Manag.* **2016**, *119*, 453–462. [[CrossRef](#)]
40. Meng, Y.-L.; Wang, B.-Y.; Li, S.-F.; Tian, S.-J.; Zhang, M.-H. Effect of calcination temperature on the activity of solid Ca/Al composite oxide-based alkaline catalyst for biodiesel production. *Bioresour. Technol.* **2013**, *128*, 305–309. [[CrossRef](#)]
41. *ASTM D6751*; Standard Specification for Biodiesel Fuel Blend Stock (B100) for Middle Distillate Fuels. ASTM International: West Conshohocken, PA, USA, 2023.
42. *EN 14214*; Read the Fuel Specifications for EN 14214-Compliant Biodiesels. Crown Oil: Bury, UK, 2014.

**Disclaimer/Publisher’s Note:** The statements, opinions and data contained in all publications are solely those of the individual author(s) and contributor(s) and not of MDPI and/or the editor(s). MDPI and/or the editor(s) disclaim responsibility for any injury to people or property resulting from any ideas, methods, instructions or products referred to in the content.